

Kerr-Newman outside a rotating de Sitter-type core: A rotating version of the Lemos-Zanchin electrically charged solution

Marcos L. W. Basso and Vilson T. Zanchin

*Centro de Ciências Naturais e Humanas, Universidade Federal do ABC,
Avenida dos Estados 5001, Santo André, São Paulo, 09210-580, Brazil*

A rotating version of the electrically charged solution of the Einstein-Maxwell system of equations modeling static regular black holes by Lemos and Zanchin [Phys. Rev. D **83**, 124005 (2011)] is obtained in the present work. The full rotating geometry consists of the Kerr-Newman exterior geometry outside a rotating de Sitter-type core with an electrically charged spheroidal shell at the boundary. To achieve this interior geometry, we utilize the Gürses-Gürsey metric and employ the Newman-Janis algorithm to generate the rotating version of the static solution. The metrics of the two spacetime regions are smoothly matched together at the rotating electrically charged shell, while the electromagnetic field satisfies the usual boundary conditions at a charged surface. Interestingly, we note that, although the Newman-Janis procedure preserves the overall electric charge of the static solution, the arbitrariness of the algorithm allows us to propose different electromagnetic fields and charge (current) distributions for the same geometry of the interior region, together with different charge (current) densities on the rotating boundary shell. For a particular choice of the interior electromagnetic field, we show that it is possible to interpret the rotating de Sitter fluid as being electrically polarized due to its rotation, despite the absence of net electric charge within the interior region, which is instead concentrated solely on the charged shell. The properties of the entire rotating solution, such as curvature regularity, energy-momentum tensor and energy conditions, are thoroughly examined in the text, revealing various types of charged rotating objects.

Keywords: Einstein-Maxwell equations; regular black holes; Kerr-Newman spacetime

I. INTRODUCTION

Regular black holes (RBH) have been a subject of great interest in the literature. Bardeen first introduced the concept of black holes with horizons however devoid of curvature singularities, postulating a suitable mass function in a spherically symmetric metric, marking the inception of regular black holes [1]. Such a mass function gives rise to a energy-momentum that was later associated with the presence of magnetic monopoles in non-linear electrodynamics [2]. At large radial coordinates, the geometry tends to the Reissner-Nordström metric, so simulating the presence of electric charge throughout the spacetime. On the other hand, in the limit of small distances, close to the center, the energy-momentum tensor tends to a perfect fluid with a de Sitter equation of state, i.e., $p = -\rho_m$. Subsequent developments in the field have largely been based on Bardeen's original proposal, with a de Sitter-type core plus some electric charge therein or elsewhere, albeit with significant advancements in implementation and analysis [3–14]. In particular, the work by Lemos and Zanchin [10] provides a brief review of the classification of regular black hole solutions through the type of junctions needed. If no junction exists, the solution remains continuous throughout the spacetime. When two spacetime regions are present, the solutions incorporate a boundary surface connecting these regions. In more extreme scenarios, the solutions entail surface layers, such as thin shells, linking the two regions. Moreover, the work [10] provides an interesting regular black hole solution, which consists of a Reissner-Nordström geometry outside a regular de Sitter-like core with an elec-

trically charged shell at the boundary. This solution, that we dub the L&Z electrically charged solution, is the focus of the present work.

While the search for RBH models have primarily focused on static configurations, efforts to explore their rotating counterparts have soon emerged. An interesting path to model such kind of rotating objects was built by following the work by Newman and Janis [16]. Furthermore, inspired by the Newman-Janis complex transformation [16], Gürses and Gürsey [15] derived a stationary and axisymmetric metric in Boyer-Lindquist coordinates, laying out a framework for constructing rotating counterparts of static and spherically symmetric solutions. This approach holds promise for devising simple models for rotating RBH. Various avenues have been pursued to elucidate the source underlying the Gürses-Gürsey metric [17, 18], and to generalize and refine the Newman-Janis algorithm [17–21].

Consequently, a substantial body of work has emerged concerning rotating regular objects [22–39]. These endeavors stem from the recognition that while the Kerr geometry [40] provides a realistic description of the exterior region of black holes with angular momentum, it presents challenges regarding the interpretation of the black hole interior, including a ring singularity and causality violations [41]. Substituting the problematic interior with a regular matter source, analogously to static RBH, offers a potential resolution. Following such strategy, the main goal of the present work consists in properly obtain and describe the rotating version of the L&Z electrically charged solution. It is worth noting that in Ref. [42], a rotating de Sitter-like metric was derived using the modified version of the Newman-Janis algorithm without com-

plexification. The resulting metric would describe the interior region of a rotating version of the L&Z static solution. However, in such a work the matching with an exterior geometry was not addressed, and the calculation of the interior electromagnetic field was omitted. In contrast, our work here presents explicit forms of all relevant quantities for the interior region and aims to establish a proper match with the exterior Kerr-Newman geometry [43] together with the electromagnetic fields.

Interestingly, we show that, although the Newman-Janis procedure preserves the overall electric charge of the static solution, the arbitrariness in constructing the Faraday-Maxwell tensor allow us to consider different types of interior electromagnetic fields together with different charge densities on the rotating shell. This result is in agreement with the investigation by Tiomno about an analogous problem in a flat spacetime [44]. Tiomno found that a charged rotating oblate ellipsoid of revolution which reproduces the exterior Kerr-Newman electromagnetic field allow different types of interior electromagnetic field with different electromagnetic materials. Moreover, the properties of the entire rotating solution, such as curvature regularity, energy-momentum tensor and energy conditions is thoroughly examined, revealing various types of objects within it.

The present work is organized as follows. In Sec. II we review the static L&Z electrically charged solution. The rotating Gürses-Gürsey geometry for charged systems is presented in Sec. III, together with its main properties. In Sec. III we discuss an important result about the nonexistence of well-behaved electromagnetic fields in the interior region without a current density. In Sec. IV we construct the rotating L&Z electrically charged solution and analyze its main properties. The different kinds of objects modeled by the complete solution are also discussed in Sec. IV. Our final comments and conclusion are made in Sec. V. Appendix A contains a brief review of the fundamental equations for Einstein-Maxwell systems, while Appendix B is dedicated to present an alternative electromagnetic field for the interior region of the rotating L&Z electrically charged solution.

II. THE LEMOS-ZANCHIN ELECTRICALLY CHARGED SOLUTION

Here we present a brief summary of the static L&Z [10] electrically charged solution. Such a solution corresponds static spherically symmetric spacetimes composed by two disjoint regions that join together at a spherical surface \mathcal{B}_r which, in Schwarzschild-like coordinates, coincides with the surface of constant radial coordinate, i.e., $\mathcal{B}_r: r = r_0 = \text{constant}$. The interior region ($r < r_0$) contains an uncharged perfect fluid obeying a de Sitter equation of state, while the exterior region ($r > r_0$) is described by the electrovacuum Reissner-Nordström (RN) solution. The surface \mathcal{B}_r bears a total electric charge q uniformly distributed over it.

The metric employed in Ref. [10] can be conveniently expressed by using Schwarzschild-like coordinates (t, r, θ, φ) as

$$ds^2 = -f(r)dt^2 + f^{-1}(r)dr^2 + r^2d\Omega^2, \quad (1)$$

where the metric potential $f(r)$ is solely a function of the radial coordinate r , and $d\Omega^2 = d\theta^2 + \sin^2\theta d\varphi^2$ represents the line element on the unit sphere.

The complete solution for the metric the form given in Eq. (1) with the function $f(r)$ defined by

$$f(r) = \begin{cases} 1 - \frac{r^2}{R^2}, & 0 \leq r \leq r_0, \\ 1 - \frac{2m}{r} + \frac{q^2}{r^2}, & r \geq r_0. \end{cases} \quad (2)$$

For convenience, the metric potential $f(r)$ is usually written as

$$f(r) = 1 - \frac{2m(r)}{r} + \frac{q^2(r)}{r^2}, \quad (3)$$

where $m(r)$ is the total inside a sphere of radius r , and is then given by

$$m(r) = \begin{cases} \frac{r^3}{2R^2}, & r < r_0, \\ m, & r \geq r_0. \end{cases} \quad (4)$$

Meanwhile, $q(r)$ is the total electric charge inside a sphere of radius r and it is given by

$$q(r) = \begin{cases} 0, & r < r_0, \\ q, & r \geq r_0. \end{cases} \quad (5)$$

The smooth matching conditions between the two spacetime metrics yield two relations for the parameters of the models. Namely,

$$\frac{m}{R} = 2\frac{r_0^3}{R^3}, \quad (6)$$

$$\frac{q}{R} = \sqrt{3}\frac{r_0^2}{R^2}. \quad (7)$$

Notice that the metric function $f(r)$ as well as its derivative $df(r)/dr$ are continuous functions across the boundary surface \mathcal{B}_r .

The interior regions contains a perfect fluid satisfying a de Sitter type equation of state, i.e., $p(r) = -\rho_m(r)$, while the exterior region is the Reissner-Nordström (RN) electrovacuum solution. The fluid quantities are given by

$$8\pi\rho_m(r) = -8\pi p(r) = \begin{cases} \frac{3}{R^2} - \frac{q^2(r)}{r^4}, & r < r_0 \\ 0, & r \geq r_0, \end{cases} \quad (8)$$

It is also convenient for future reference to write the complete solution for the electromagnetic quantities of

the L&Z solutions here. The charge density profile may be written as

$$\rho_e(r) = \frac{q}{4\pi r_0^2} \delta(r - r_0), \quad (9)$$

where $\delta(r - r_0)$ stands for the Dirac delta function, so indicating that the total charge is distributed uniformly over the boundary surface \mathcal{B}_r . Therefore, the electric potential $\phi(r)$ is given by

$$\phi(r) = \begin{cases} \frac{q}{r_0}, & 0 \leq r < r_0, \\ \frac{q}{r}, & r \geq r_0, \end{cases} \quad (10)$$

while the electric field $E(r)$ presents a jump at $r = r_0$, i.e.,

$$E(r) = \begin{cases} 0, & 0 \leq r < r_0, \\ \frac{q}{r^2}, & r \geq r_0. \end{cases} \quad (11)$$

As it can be seen, the matching conditions for the gauge potential and for the electromagnetic field are $[\mathcal{A}_a] = 0$, $[F_{ab}] = 0$, and $[F_{an}] = 4\pi\sigma_e u_a$, where σ_e and u_a represent the proper surface charge density and the proper four velocity of the shell, respectively. The jump in the normal component of the electromagnetic field yields the surface charge density of the boundary surface, $\sigma_e = q/(4\pi r_0^2)$.

III. THE GÜRSSES-GÜRSEY METRIC AND THE ELECTROMAGNETIC FIELD

A. The Gürses-Gürsey metric

Gürses-Gürsey [15] were able to show that the Newman-Janis algorithm [16] belongs to the Trautman-Newman class of complex coordinate translations that works for the algebraically special metrics of the Kerr-Schild class. By starting from the spherical seed metric in Eq. (1), the Gürses-Gürsey approach yields a rotating and axially-symmetric metric that, in Boyer-Lindquist coordinates (t, r, θ, φ) , takes the form

$$ds^2 = - \left(1 - \frac{2r M(r)}{\Sigma}\right) dt^2 + \frac{\Sigma}{\Delta(r)} dr^2 + \Sigma d\theta^2 - \frac{4r M(r) a \sin^2 \theta}{\Sigma(r, \theta)} dt d\varphi + \left(r^2 + a^2 + \frac{2r M(r) a^2 \sin^2 \theta}{\Sigma(r, \theta)}\right) \sin^2 \theta d\varphi^2, \quad (12)$$

where a is the rotation parameter, and the functions $M(r)$, $\Sigma(r, \theta)$, and $\Delta(r)$ are defined as

$$M(r) = m(r) - q^2(r)/2, \quad (13)$$

$$\Sigma(r, \theta) \equiv \Sigma = r^2 + a^2 \cos^2 \theta, \quad (14)$$

$$\Delta(r) \equiv \Delta = r^2 + a^2 - 2r M(r), \quad (15)$$

respectively. In our case, the mass function $m(r)$ and the charge function $q(r)$ are given by Eqs. (4) and (5), respectively.

As well know, metric (12) reproduces the Kerr-Newman (KN) geometry in the case of constant $m(r) = m$ and constant $q(r) = q$, so that $M(r) = m - q^2/(2r)$. In the case of nonconstant $m(r)$ and $q(r)$, it describes a spacetime region fulfilled with charged matter. As discussed in our previous work [45], the metric with nonconstant $m(r)$ and $q(r)$ can be used to describe an interior spacetime region (\mathcal{M}_-) that may be joined to the KN metric, with the KN metric describing the exterior electrovacuum spacetime region (\mathcal{M}_+). However, other very interesting situation is the one we are interested here, namely, the case where the interior spacetime region \mathcal{M}_- is described by (12) with nonconstant $m(r) = r^3/(2R^2)$ but with zero electric charge $q(r) = 0$, that is joined to the exterior electrovacuum KN region \mathcal{M}_+ . Such a matching is possible by adding some electric charge on the matching surface.

B. On the nonexistence of well-behaved electromagnetic fields with vanishing current density

In order to properly generalize the L&Z solution for the rotating case and describe its possible interior electromagnetic fields, we discuss the nonexistence of well-behaved electromagnetic fields in the interior region without a current density, unless the electromagnetic fields completely vanish in the interior region.

Let us start by writing the Maxwell equations (see Eqs. (A2) and (A3) in Appendix A) for the Gürses-Gürsey metric (12) with vanishing current density, $J^\mu = 0$. First, notice that the nontrivial components of a stationary and axially symmetric Faraday-Maxwell tensor in Boyer-Lindquist coordinates are F_{rt} , $F_{\theta t}$, $F_{r\varphi}$ and $F_{\theta\varphi}$. Hence, the Maxwell equations are given by

$$\begin{aligned} \partial_r [(r^2 + a^2) \sin \theta F_{rt}] + \partial_\theta [\sin \theta F_{\theta t}] &= 0, \\ \partial_r [\csc \theta F_{r\varphi}] + \partial_\theta \left[\frac{\csc \theta}{r^2 + a^2} F_{\theta\varphi} \right] &= 0, \\ \partial_r F_{\theta t} - \partial_\theta F_{rt} &= 0, \\ \partial_r F_{\theta\varphi} - \partial_\theta F_{r\varphi} &= 0, \end{aligned} \quad (16)$$

where $\partial_\mu \equiv \partial/\partial x^\mu$. It is worth mentioning that we do not assume any previous form for the components of the Faraday-Maxwell tensor.

By noticing that, for the metric (12), the nontrivial components of the Faraday-Maxwell tensor are related by

$$F_{r\varphi} = -a \sin^2 \theta F_{rt}, \quad a F_{\theta\varphi} = -(r^2 + a^2) F_{\theta t}, \quad (17)$$

we can rewrite the Maxwell equations (16) in terms of

the components F_{rt} and $F_{\theta t}$ only, i.e.,

$$\partial_r [(r^2 + a^2) \sin \theta F_{rt}] + \partial_\theta [\sin \theta F_{\theta t}] = 0, \quad (18)$$

$$\partial_r [a \sin \theta F_{rt}] + \partial_\theta \left[\frac{\csc \theta}{a} F_{\theta t} \right] = 0, \quad (19)$$

$$\partial_r F_{\theta t} - \partial_\theta F_{rt} = 0, \quad (20)$$

$$\partial_r [(r^2 + a^2) F_{\theta t}] - \partial_\theta [a^2 \sin^2 \theta F_{rt}] = 0. \quad (21)$$

Here we follow closely the work by Dymnikova and Galaktionov [49]. By manipulating Eqs. (18) and (19) it is possible to obtain the following set of equations

$$\frac{\partial}{\partial \theta} \left[\frac{\partial}{\partial r} \left(\frac{\Sigma}{r \sin \theta} F_{\theta t} \right) + \frac{2F_{\theta t}}{\sin \theta} \right] = 0, \quad (22)$$

$$F_{rt} = \frac{1}{2a^2 r \sin \theta} \frac{\partial}{\partial \theta} \left(\frac{\Sigma}{\sin \theta} F_{\theta t} \right). \quad (23)$$

The integration of Eq. (22) in variable θ furnishes the relation

$$\frac{\partial}{\partial r} \left(\frac{\Sigma}{r \sin \theta} F_{\theta t} \right) + \frac{2F_{\theta t}}{\sin \theta} = \Phi(r), \quad (24)$$

where $\Phi(r)$ is an arbitrary integration function that depends on the coordinate r alone. Moreover, by introducing the function $V_{\theta t} = \Sigma F_{\theta t}/(r \sin \theta)$, Eq. (24) may be recast into the following differential equation

$$\frac{\partial}{\partial r} V_{\theta t} + \frac{2r}{\Sigma} V_{\theta t} = \Phi(r), \quad (25)$$

which can be easily solved and give us

$$V_{\theta t} = \Sigma^{-1} \left(\int \Sigma \Phi(r) dr + \Psi(\theta) \right), \quad (26)$$

where $\Psi(\theta)$ is another integration function that depends on the coordinate θ alone. From this, we can completely describe the components F_{rt} and $F_{\theta t}$ in terms of the integration functions $\Phi(r)$ and $\Psi(\theta)$, i.e.,

$$F_{rt} = \frac{\csc^2 \theta}{2a^2 \Sigma^2} \left[\Sigma \hat{\Psi}(\theta) - \Psi(\theta) \tan \theta (\Sigma - 2a^2 \sin^2 \theta) \right] + \frac{\cos \theta}{\Sigma^2} \left(\int \Phi(r) r^2 dr - r^2 \int \Phi(r) dr \right), \quad (27)$$

$$F_{\theta t} = \frac{r}{\Sigma^2} \Psi(\theta) + \frac{r \sin \theta}{\Sigma^2} \int \Sigma \Phi(r) dr, \quad (28)$$

where the overhat ($\hat{\cdot}$) denotes differentiation with respect to the coordinate θ .

The integration functions $\Phi(r)$ and $\Psi(\theta)$ can be determined by the remaining Maxwell Eqs. (20) and (21). The remaining Maxwell equations can be put in the form

$$\frac{\partial}{\partial r} \left[\frac{\partial}{\partial \theta} \left(\frac{\Sigma}{\sin 2\theta} F_{\theta t} \right) - a^2 F_{\theta t} \right] = 0, \quad (29)$$

$$F_{rt} = \frac{1}{a^2 \sin 2\theta} \frac{\partial}{\partial r} [(r^2 + a^2) F_{\theta t}], \quad (30)$$

which, from the expressions (27) and (28), we get, after a tedious but straightforward calculation, the following equations for the integration functions

$$\begin{aligned} \sin \theta (\Phi(r) r^2)' &= 0, \\ \hat{\Psi}(\theta) + (\tan \theta - \cot \theta) \Psi(\theta) - \sin \theta \tan \theta (r \Sigma \Phi(r) & \\ - \int \Phi(r) r^2 dr) - a^2 \sin^2 \theta \cos \theta \int \Phi(r) dr &= 0, \end{aligned} \quad (31)$$

where the prime ($'$) denotes differentiation with respect to the coordinate r . The above equations can be easily integrated to give

$$\Phi(r) = A r^{-2}, \quad (32)$$

$$\Psi(\theta) = B \sin 2\theta, \quad (33)$$

with A and B being integration constants. Hence, substituting these functions into Eqs. (27) and (28), we get the general expression for the electromagnetic fields with no current density in the Gürses-Gürsey geometry as

$$F_{rt} = \frac{2Ar \cos \theta}{\Sigma^2} - \frac{B(r^2 - a^2 \cos^2 \theta)}{a^2 \Sigma^2}, \quad (34)$$

$$F_{\theta t} = \frac{A \sin \theta (r^2 - a^2 \cos^2 \theta)}{\Sigma^2} + \frac{Br \sin 2\theta}{\Sigma^2}. \quad (35)$$

We first notice that the well-known Kerr-Newman electromagnetic field is recovered by choosing $A = 0$ and $B = -qa^2$. The second important fact to notice is that, for any nonzero arbitrary constants A and B , the electromagnetic field is not well-behaved at the ring ($r = 0, \theta = \pi/2$). Indeed,

$$\lim_{r \rightarrow 0} \left(\lim_{\theta \rightarrow \pi/2} F_{rt} \right) = - \lim_{r \rightarrow 0} \frac{B}{a^2 r^4} \rightarrow -\infty, \quad (36)$$

$$\lim_{r \rightarrow 0} \left(\lim_{\theta \rightarrow \pi/2} F_{\theta t} \right) = \lim_{r \rightarrow 0} \frac{A}{r^4} \rightarrow -\infty. \quad (37)$$

As a conclusion, the electromagnetic field is well-behaved only if they vanish completely in the interior, what happens by taking $A = 0$ and $B = 0$. In such a case, if trying to match them with the Kerr-Newman exterior electromagnetic field, the tangential components of the Faraday-Maxwell tensor are discontinuous across the boundary.

C. The energy-momentum tensor of the Gürses-Gürsey metric

As usual, the energy-momentum tensor (EMT) that sources the rotating Gürses-Gürsey geometry can be decomposed through the Carter's orthonormal tetrad,

$$\begin{aligned} e_0^\mu &= \frac{1}{\sqrt{\pm \Delta \Sigma}} [(r^2 + a^2) \delta_t^\mu + a \delta_\varphi^\mu], \\ e_1^\mu &= \sqrt{\frac{\pm \Delta}{\Sigma}} \delta_r^\mu, \quad e_2^\mu = \frac{1}{\sqrt{\Sigma}} \delta_\theta^\mu, \\ e_3^\mu &= \frac{1}{\sqrt{\Sigma} \sin \theta} [a \sin^2 \theta \delta_t^\mu + \delta_\varphi^\mu], \end{aligned} \quad (38)$$

where the \pm signs preceding Δ are to be chosen as to guarantee the tetrad components are real numbers. The positive sign is chosen for spacetime regions where $\Delta > 0$, while the negative sign is chosen for spacetime regions where $\Delta < 0$.

Hence, the EMT can be recast into the form

$$T^{\mu\nu} = \varrho e_0^\mu e_0^\nu + \mathfrak{p}_1 e_1^\mu e_1^\nu + \mathfrak{p}_2 e_2^\mu e_2^\nu + \mathfrak{p}_3 e_3^\mu e_3^\nu, \quad (39)$$

where ϱ , p_r , p_θ and p_φ are the total energy density, the radial, and the tangential pressures of the fluid, respectively. Such quantities are given by [17]

$$\varrho(r, \theta) = -\mathfrak{p}_1(r, \theta) = \frac{r^2 M'(r)}{4\pi \Sigma^2}, \quad (40)$$

$$\mathfrak{p}_2(r, \theta) = \mathfrak{p}_3(r, \theta) = \frac{r^2 M'(r)}{4\pi \Sigma^2} - \frac{1}{8\pi \Sigma} \left(r M(r) \right)'', \quad (41)$$

where the primes indicate derivatives with respect to the coordinate r .

Given that we are dealing with charged matter, the EMT described by Eq. (39) can be decomposed into $T_{\mu\nu} = M_{\mu\nu} + E_{\mu\nu}$, as described in Appendix A, where $M_{\mu\nu}$ represents the EMT of the matter fluid alone and $E_{\mu\nu}$ represents the EMT of the electromagnetic field. The projection of the electromagnetic EMT onto the Carter's orthonormal frame yields the following nonvanishing components

$$\begin{aligned} \varrho_{em}(r, \theta) &\equiv E_{\mu\nu} e_0^\mu e_0^\nu = \frac{1}{8\pi} \left(F_{rt}^2 + \frac{F_{\theta t}^2}{a^2 \sin^2 \theta} \right), \\ \mathfrak{p}_{em1}(r, \theta) &\equiv E_{\mu\nu} e_1^\mu e_1^\nu = -\varrho_{em}(r, \theta), \\ \mathfrak{p}_{em2}(r, \theta) &\equiv E_{\mu\nu} e_2^\mu e_2^\nu = \varrho_{em}(r, \theta), \\ \mathfrak{p}_{em3}(r, \theta) &\equiv E_{\mu\nu} e_3^\mu e_3^\nu = \varrho_{em}(r, \theta). \end{aligned} \quad (42)$$

Then, it is easy to see that the EMT of the matter can be determined by the difference between the total EMT and the electromagnetic EMT, i.e., $M_{\mu\nu} e_a^\mu e_b^\nu = (T_{\mu\nu} - E_{\mu\nu}) e_a^\mu e_b^\nu$, and it corresponds to the EMT of a non-isotropic matter fluid since

$$\begin{aligned} \varrho_m(r, \theta) &\equiv M_{\mu\nu} e_0^\mu e_0^\nu = \varrho(r, \theta) - \varrho_{em}(r, \theta), \\ \mathfrak{p}_{m1}(r, \theta) &\equiv M_{\mu\nu} e_1^\mu e_1^\nu = -\varrho(r, \theta) + \varrho_{em}(r, \theta), \\ \mathfrak{p}_{m2}(r, \theta) &\equiv M_{\mu\nu} e_2^\mu e_2^\nu = \mathfrak{p}_2(r, \theta) - \varrho_{em}(r, \theta), \\ \mathfrak{p}_{m3}(r, \theta) &\equiv M_{\mu\nu} e_3^\mu e_3^\nu = \mathfrak{p}_2(r, \theta) - \varrho_{em}(r, \theta). \end{aligned} \quad (43)$$

These relations are going to be used in the next section.

D. The electric and magnetic fields decomposition and the total charge

It is useful to decompose the Faraday-Maxwell Faraday-Maxwell tensor $F_{\mu\nu}$ in terms of its electric and magnetic components relative to a given observer. As well-known, the electric and magnetic fields as measured by the comoving observer with the fluid are given by

$$\begin{aligned} E_\mu &= F_{\mu\nu} u^\nu, \\ B_\mu &= \frac{1}{2} \epsilon_{\nu\mu\alpha\beta} u^\nu F^{\alpha\beta}, \end{aligned} \quad (44)$$

where u^μ is the four-velocity of the comoving observer, which, in the present case, is given by the first element of the Carter tetrad in Eq. (38), $u^\mu = e_0^\mu$, and $\epsilon_{\beta\mu\nu\alpha}$ is the usual four-dimensional Levi-Civita tensor. After the definitions in (44), the Faraday-Maxwell decomposes in the form

$$F_{\mu\nu} = u_\mu E_\nu - u_\nu E_\mu + \epsilon_{\mu\nu\alpha} B^\alpha, \quad (45)$$

where $\epsilon_{\mu\nu\alpha} = \epsilon_{\beta\mu\nu\alpha} u^\beta$ is the three-dimensional Levi-Civita tensor defined in the subspace orthogonal to the comoving observer.

By using the relation between the components of the Faraday-Maxwell tensor form Eq. (17) and the projections Eq. (44), a straightforward calculation shows that the only nonzero components of the electric and magnetic fields are

$$E_r = \sqrt{\frac{\Sigma}{\pm\Delta}} F_{rt}, \quad B_r = -\sqrt{\frac{\Sigma}{\pm\Delta}} \frac{F_{\theta t}}{a \sin \theta}. \quad (46)$$

A noteworthy feature here is that, as perceived by the comoving observer, the electric and the magnetic fields are parallel to each other. This was already noticed by Tiomno [44] and Lynden-Bell [46] for the flat spacetime limit of the Kerr-Newman electromagnetic field. In addition, Gair and Lynden-Bell [47] also verified that, considering electromagnetic fields in Carter separable spacetimes, there exists an observer for every spheroidal surface such that the electric and magnetic fields as measured in this frame are parallel to each other.

Finally, other important quantity for the present analysis is the total electric charge inside a surface of constant coordinate r . Given the hyper-surface Σ_t defined by $t = \text{constant}$, we can calculate the total charge $q(r)$ inside a spheroid of constant r through the volume integral

$$q(r) = - \int_{\Sigma_t} J^\mu \eta_\mu dV = - \frac{1}{4\pi} \int_{\Sigma_t} \nabla_\nu F^{\mu\nu} \eta_\mu dV, \quad (47)$$

where η_μ is a unitary time-like vector orthogonal to the surface Σ_t , and $dV = \sqrt{h} dr d\theta d\varphi$, with h being the determinant of the induced metric in Σ_t . A straightforward calculation shows that

$$\begin{aligned} q(r) &= \frac{1}{2} \int_0^r dr' \int_0^\pi d\theta \partial_\nu (\sqrt{-g} F^{t\nu}) \\ &= \frac{1}{2} \int_0^r dr' \int_0^\pi d\theta \partial_{r'} [(r'^2 + a^2) \sin \theta F_{rt}] \\ &= \frac{1}{2} \int_0^\pi [(r'^2 + a^2) \sin \theta F_{rt}]_0^r d\theta, \end{aligned} \quad (48)$$

where we used the fact that $\sqrt{-g} F^{tr} = (r^2 + a^2) \sin \theta F_{rt}$, and the θ -component on the summation when integrated over the polar angle does not contribute.

IV. A ROTATING VERSION OF THE LEMOS-ZANCHIN ELECTRICALLY CHARGED SOLUTION: KERR-NEWMAN OUTSIDE A ROTATING DE SITTER-TYPE CORE

A. Preliminary remarks

By following the procedure to get the Gürsey-Gürses metric from a static seed metric, as summarized in Sec. III A, we obtain here a rotating version of the electrically charged solution by Lemos and Zanchin [10]. As we briefly reviewed in Sec. II, the complete static seed geometry consists of a Reissner-Nordström solution outside a de Sitter core, with an electrically charged shell binding the two spacetime regions.

Such a metric is, in principle, an interior rotating geometry for the static interior de Sitter core of the L&Z solution.

At this point, it is worth mentioning the rotating metric obtained in Ref. [42] through a modified version of the Newman-Janis algorithm without complexification. Such a metric is, in principle, an interior rotating geometry taking the interior de Sitter core of the L&Z solution as the static seed metric. However, the matching with an exterior geometry was not provided in [42], and the interior electromagnetic field was not calculated either. In contrast, here we present the explicit forms of all the relevant quantities for the interior region, and shall provide a proper match to the exterior Kerr-Newman geometry and electromagnetic fields.

B. The interior rotating solution

The interior solution for the metric is characterized by the Gürses-Gürsey metric (12) with the mass function $M(r)$ given by

$$M(r) = m(r) = \frac{r^3}{2R^2}. \quad (49)$$

In order to define electromagnetic gauge potential, let us recall that, in the interior region of the L&Z static solution, the electric potential is constant and given by $\phi(r) = q/r_0$, and the net charge inside any sphere of constant radius $r < r_0$ is zero. Hence, a possible form of the electromagnetic gauge potential \mathcal{A}_μ , which is consistent with the geometry (12), is constant along the coordinate r , and also leads to a vanishing net charge inside a spheroid of constant radius $r < r_0$, is given by

$$\mathcal{A}_\mu = -\frac{qr_0}{\Sigma_0} (\delta_\mu^t - a \sin^2 \theta \delta_\mu^\varphi), \quad (50)$$

with $\Sigma_0 = r_0^2 + a^2 \cos^2 \theta$. Notice that the gauge potential (50) depends on the polar coordinate θ alone.

In this case, from Eq. (50), we have $F_{rt} = 0 = F_{r\varphi}$ and the nontrivial components of the Faraday-Maxwell

tensor are

$$\begin{aligned} F_{\theta t} &= -\frac{qr_0 a^2 \sin 2\theta}{\Sigma_0^2}, \\ F_{\theta\varphi} &= -\frac{(r_0^2 + a^2)}{a} F_{\theta t}. \end{aligned} \quad (51)$$

It is easy to verify that these two components of $F_{\mu\nu}$ vanish in the limit $a \rightarrow 0$, recovering the static L&Z solution. It also can be seen from the result (51) that the Faraday-Maxwell tensor is well-behaved in the whole interior region, being finite everywhere inside the fluid. In particular, all components of $F_{\mu\nu}$ vanish for $\theta = 0$ and for $\theta = \pi/2$ for all $r < r_0$, including the ring S^1 : ($r = 0$, $\theta = \pi/2$).

Interestingly, we notice that, once the electric field is vanishing, $E_\mu = F_{\mu\nu} u^\nu = 0$, the fluid behaves like a perfect conductor, in agreement with the results found by Tiomno [44] for the interior material that reproduces the exterior Kerr-Newman electromagnetic field in flat spacetime. In fact, from Eq. (46) and the vanishing of F_{rt} in the interior region, it follows that the radial component of the electric field E_r vanishes, while the radial component of the magnetic field is given by

$$B_r = \sqrt{\frac{\Sigma}{\pm\Delta}} \frac{2qr_0 a \cos \theta}{\Sigma_0^2}. \quad (52)$$

The current density in the interior region that results from the Faraday-Maxwell field (B4) is given by

$$\begin{aligned} J^t &= \frac{qr_0 a^2}{2\pi \Sigma_0^4} [(r_0^2 - 3a^2 \cos^2 \theta) \sin^2 \theta - 2\Sigma_0 \cos^2 \theta], \\ J^\varphi &= \frac{qr_0 a}{2\pi \Sigma_0^4} (r_0^2 - 3a^2 \cos^2 \theta), \end{aligned} \quad (53)$$

with the other components being identically zero. As it seen from Eq. (53), the two nontrivial components of the current density are finite everywhere in the interior region, even at the ring S^1 and at the disc ($r = 0$, $0 \leq \theta < \pi/2$).

Figure 1 show the behavior of while J^t as a function of θ for a few values of the rotation parameter a/r_0 . As it seen from that figure, J^t is negative near the poles ($\theta = 0, \pi$), while J^t is positive near the equator $\theta = \pi/2$, indicating that the medium in that region is electrically polarized. Moreover, we can infer that such a polarization is induced by the rotation of the de Sitter-like fluid in the presence of the charged rotating spheroidal shell, once $J^t \rightarrow 0$ for $a \rightarrow 0$.

As expected, the electromagnetic field does not vanish in the interior region, since here we have a rotating spheroidal charged shell that induces electric and magnetic fields also in its interior. Such a electromagnetic field gives rise to a current density, and then we may interpret the matter content of that region as a charged rotating de Sitter-like fluid. However, since the induced electromagnetic field is such $F_{rt} = 0$, it follows from

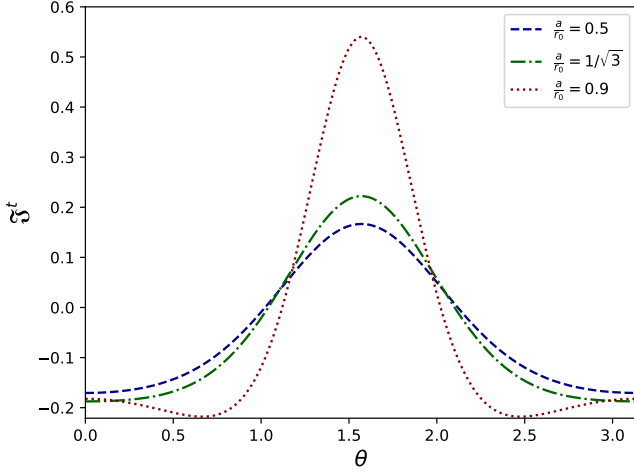


Figure 1. The normalized t -component of the current density $\mathfrak{J}^t = J^t/(4\pi q r_0^3/3)$ as a function of θ for different values of a/r_0 .

Eq. (48) that the net electric charge inside any spheroid of radius $r = r_0$ vanishes, i.e., $\mathbf{q}(r_0) = 0$.

We may refine the analysis of the charge distribution within the fluid by considering a comoving observer in that region.

The four velocity u^μ of such a comoving observer with the fluid coincides with the first element of the Carter tetrad (38), i.e., $u^\mu = e_0^\mu$. Then, the four-current density J^μ may be decomposed as

$$J^\mu = \rho_e u^\mu + j^\mu, \quad (54)$$

where

$$\begin{aligned} \rho_e &= -J^\mu u_\mu, \\ j^\mu &= (u^\mu u_\nu + \delta^\mu_\nu) J^\nu, \end{aligned} \quad (55)$$

with e_3^μ standing for the fourth component of the Carter tetrad (38). The quantities defined in (55) are interpreted as the charge density and the conduction current density as measured by such an observer, respectively. In the present case, they reduce to

$$\rho_e = -\sqrt{\frac{\pm\Delta}{\Sigma}} \frac{q r_0 a^2 \cos^2 \theta}{\pi \Sigma_0^3}, \quad (56)$$

$$j^\mu = \frac{q r_0 a (r_0^2 - a^2 \cos^2 \theta)}{2\pi \Sigma_0^3} \frac{a \sin \theta}{\sqrt{\Sigma}} e_3^\mu. \quad (57)$$

Thus, the nonzero spatial current can exist alongside a zero electric field, provided the medium has infinite conductivity [48].

It is worth mentioning once again that a different gauge potential yields a different result also for the net charge inside the fluid. An alternative electromagnetic field for the rotating L&Z electrically charged solution is analyzed in Appendix B.

C. The exterior rotating solution

The exterior solution is characterized by the Gürses-Gürsey metric (12) with the mass function $M(r)$ given by

$$M(r) = m - \frac{q^2}{2r}. \quad (58)$$

Therefore, our exterior solution is the well-known Kerr-Newman solution [43], with the electromagnetic gauge potential given by

$$\mathcal{A}_\mu = -\frac{q r}{\Sigma} (\delta_\mu^t - a \sin^2 \theta \delta_\mu^\varphi), \quad (59)$$

from which the nontrivial components for the Faraday-Maxwell tensor are obtained,

$$\begin{aligned} F_{rt} &= \frac{q (r^2 - a^2 \cos^2 \theta)}{\Sigma^2}, \\ F_{\theta t} &= -\frac{q r a^2 \sin 2\theta}{\Sigma^2}, \\ F_{r\varphi} &= -a \sin^2 \theta F_{rt}, \\ F_{\theta\varphi} &= -\frac{(r^2 + a^2)}{a} F_{\theta t}. \end{aligned} \quad (60)$$

D. Matching conditions

Moving on to the matching conditions, the interior region \mathcal{M}_- corresponds to $r < r_0$, while the exterior region \mathcal{M}_+ corresponds to $r_0 < r < \infty$. We first address the metric junction conditions using the Darmois-Israel (DI) approach [50], followed by the matching conditions of the electromagnetic field.

The boundary between the two spacetime regions is the surface \mathcal{B}_r defined by $r = r_0 = \text{constant}$. Then, let $\xi^a \equiv (\tau, \theta, \varphi)$ be the coordinates in \mathcal{B}_r , and $x_\pm^\mu \equiv (t_\pm, r_\pm, \theta_\pm, \varphi_\pm)$ be the coordinates of regions \mathcal{M}_- and \mathcal{M}_+ , respectively. Notice that, due to the symmetry of the spacetime and of the boundary surface, and since we are considering smooth boundary conditions for the geometric quantities, the coordinates of the two spacetime regions may be identified, i.e., $t_- = t_+$, $r_- = r_+$, $\theta_- = \theta_+ = \theta$, and $\varphi_- = \varphi_+ = \varphi$. Hence, from now on we drop the \pm indexes. The DI approach deals with the first and the second fundamental forms on \mathcal{B}_r , h_{ab} and K_{ab} , respectively. These geometric objects are defined in terms of four-dimensional geometric objects via the well-known relations $h_{ab} = \varepsilon_a^\mu \varepsilon_b^\nu g_{\mu\nu}$ and $K_{ab} = \varepsilon_a^\mu \varepsilon_b^\nu \nabla_\nu n_\mu$, where $\varepsilon_a^\mu = \partial x^\mu / \partial \xi^a$. Here, $n_\mu = \sqrt{g_{rr}} \delta_\mu^r$ denotes the unit normal vector to the surface \mathcal{B}_r .

The assumption a smooth transition between the two spacetime regions across the boundary \mathcal{B}_r , i.e., $[h_{ab}] = 0$

and $[K_{ab}] = 0$, furnishes

$$\frac{1}{R^2} = \frac{1}{r_0^3} \left(2m - \frac{q^2}{r_0} \right), \quad (61)$$

$$\frac{1}{R^2} = -\frac{1}{r_0^3} \left(m - \frac{q^2}{r_0} \right), \quad (62)$$

which implies in Eqs. (6) and (7), being the same constraints found in the static solution.

Similarly to the static L&Z solution, the Faraday-Maxwell tensor is not continuous across the boundary, requiring a charged shell. The matching conditions for the gauge potential and the electromagnetic field tensor are thus given by

$$\begin{aligned} [A_a] &= [\varepsilon_a^\mu A_\mu] = 0, \\ [F_{ab}] &= [\varepsilon_a^\mu \varepsilon_b^\nu F_{\mu\nu}] = 0, \\ [F_{an}] &= [\varepsilon_a^\mu n^\nu F_{\mu\nu}] = 4\pi\sigma_e u_a, \end{aligned} \quad (63)$$

where σ_e is the surface charge density and u^a is the four-velocity of the boundary shell given by the e_0^μ element of the Carter tetrad (38).

It is straightforward to see that the first two conditions in Eq. (63) are trivially satisfied, while the last condition gives us the charge density of the shell as measured by an observer comoving with the boundary, i.e.,

$$\sigma_e = \frac{q(r_0^2 - a^2 \cos^2 \theta)}{4\pi\Sigma_0^2}. \quad (64)$$

Let us notice that the result for the static solution (9) is recovered form (64) in the limit $a = 0$. In addition, we can see that the charge density of the shell may change its sign depending on the values of r_0/a , being positive for $\cos\theta < r_0/a$ and negative for $\cos\theta > r_0/a$, which implies that the charge density of the shell is also electrically polarized.

The integration of the charge density (64) along the surface $r = r_0$ gives the result q . Moreover, as already mention, the integration of the component J^t of the current density given in Eq. (53) over the whole interior region gives zero, confirming that the total charge of the distribution is exactly q , as expected. Therefore, we can think of the rotating de Sitter fluid in the interior region as being electrically polarized due to rotation.

E. Curvature regularity

It is pertinent to note that, as shown by Torres [28] and Maeda [36], the Gürses-Gürsey metric with mass functions of the form $M(r) = m_0 r^{3+\alpha}$ for $\alpha \geq 0$, upon extension to $r < 0$, exhibits a ring-like conical singularity at the ring S^1 , rather than a scalar polynomial curvature singularity like the Kerr and Kerr-Newman spacetimes. On the other hand, as also shown by Torres [38], if the extension to $r < 0$ is not carried out, the ring S^1 is also devoid of conical singularity. In the present case, for the

interior region, where the ring is located, the mass function is given by Eq. (49), i.e., the mass function is of the form $m_0 r^{3+\alpha}$ with $\alpha = 0$, and the extension to $r < 0$ is not performed, implying that the ring S^1 does not correspond to any kind of singularity.

However, as noticed in several investigations [22, 23, 28, 32, 36], even when assuming finite values at the ring, the curvature scalars are not well-defined there for $\alpha = 0$. This is because the curvature scalars are functions that depend on the path taken when approaching the ring. This phenomenon also occurs in the present case.

F. The energy-momentum tensor

1. Interior energy-momentum tensor

Utilizing Carter's orthonormal tetrad as defined in Eq.(38), the total EMT acquires a diagonal structure $T_{\mu\nu} e_a^\mu e_b^\nu = \text{diag}(\varrho, \mathfrak{p}_1, \mathfrak{p}_2, \mathfrak{p}_3)$. The eigenvalues ϱ and \mathfrak{p}_1 are interpreted as the total energy density and the effective radial pressure, respectively. The eigenvalues \mathfrak{p}_2 and \mathfrak{p}_3 are the effective tangential pressures. Equations (40) and (41), together with the mass function given by Eq. (49), lead to the following expressions for the eigenvalues,

$$\begin{aligned} \varrho = -\mathfrak{p}_1 &= \frac{3}{8\pi R^2} \frac{r^4}{\Sigma^2}, \\ \mathfrak{p}_2 = \mathfrak{p}_3 &= \frac{3}{8\pi R^2} \frac{r^4}{\Sigma^2} \left(1 - \frac{2\Sigma}{r^2} \right). \end{aligned} \quad (65)$$

Notice that, in the limit $r \rightarrow 0$, the energy density and pressures present the same behavior as the curvature scalars analyzed in the previous section.

The contribution of the electromagnetic field to the EMT are obtained from Eqs. (42) and (51), in which it is enough to calculate the energy density as measured by the Carter's frame, namely,

$$\varrho_{em} = \frac{4q^2 r_0^2 a^2 \cos^2 \theta}{8\pi\Sigma_0^4}, \quad (66)$$

$$\mathfrak{p}_{em2} = \mathfrak{p}_{em3} = -\mathfrak{p}_{em1} = \varrho_{em}.$$

In this case, the EMT of the electromagnetic field alone is not continuous across the boundary r_0 due to the charged shell. Moreover, we can see that the energy density and pressures depend only on the coordinate θ and vanish for $\theta = \pi/2$.

The matter contribution to the energy density and pressures can be obtained by subtracting $E_{\mu\nu}$ from $T_{\mu\nu}$. In the Carter's frame, the eigenvalues of the matter EMT are given by

$$\begin{aligned} 8\pi\varrho_m = -8\pi\mathfrak{p}_{m1} &= \frac{3m}{2r_0^3} \left(\frac{r^4}{\Sigma^2} - \frac{4r_0^6 a^2 \cos^2 \theta}{\Sigma_0^4} \right), \\ 8\pi\mathfrak{p}_{m2} = 8\pi\mathfrak{p}_{m3} &= 8\pi\varrho_m - \frac{3mr^2}{r_0^3 \Sigma}, \end{aligned} \quad (67)$$

which represents a non-isotropic fluid.

2. Exterior energy-momentum tensor

Finally, by using the relation in Eq. (41), together with the mass function $m(r) = m - q^2/2r$, we obtain the explicit expressions for the eigenvalues valid in the exterior region \mathcal{M}_+ . Namely,

$$\begin{aligned} 8\pi\rho &= -8\pi p_1 = \frac{3mr^4}{r_0^3\Sigma^2} = \frac{q^2}{\Sigma^2}, \\ 8\pi p_2 &= 8\pi p_3 = 8\pi\rho_+ = \frac{q^2}{\Sigma^2}, \end{aligned} \quad (68)$$

that is due to the presence of the electromagnetic vacuum field.

It is worth noticing that the total EMT is continuous across the boundary $r = r_0$. This is easily seen by comparing the relations for the energy density and pressures in Eq. (65) to the corresponding relations in Eq. (68).

G. Energy conditions

In [28], Torres demonstrated that if the mass function $m(r)$ of the Gürses-Gürsey metric can be expanded as a Taylor polynomial series around $r = 0$, then the weak energy condition should be violated near $r = 0$. Additionally, Maeda [36] extended Torres findings by showing that if the mass function $m(r)$ can be expanded around the locus $r = 0$, with $\theta \neq \pi/2$, as $M(r) \approx m_0 r^{3+\alpha}$ with $\alpha \geq 0$, then all energy conditions are violated in the vicinity of $r = 0$ for $m_0 > 0$, while the null energy condition and the strong energy condition hold for $m_0 < 0$. Consequently, given that, in our case, the mass function is given by Eq. (49), yielding $m_0 = R^{-2}/2 > 0$, it becomes evident that all the energy conditions are infringed around the region $r = 0$, $\theta \neq \pi/2$.

H. On the horizons and ergosurfaces of the rotating geometry

The matching conditions $Rq = \sqrt{3}r_0^2$ and $R^2m = 2r_0^3$ in Eq. (15) allow us to obtain the horizons radii r_h as the real and positive roots of the polynomial equations

$$\begin{aligned} \Delta_-(r) &= r^2 + a^2 - \frac{m}{2r_0^3}r^4 = 0, \\ \Delta_+(r) &= r^2 + a^2 - 2mr + \frac{3mr_0}{2} = 0, \end{aligned} \quad (69)$$

with the supplemental conditions that the horizons are represented by the roots of $\Delta_-(r)$ if $r_h \leq r_0$, while, for $r_h \geq r_0$, the horizons are represented by the roots $\Delta_+(r)$. These polynomial equations can be easily solved in terms

of radicals and the solutions are given by

$$\begin{aligned} r_{k-} &= r_0 \sqrt{\frac{r_0}{m} \left(1 + (-1)^k \sqrt{1 + \frac{2m a^2}{r_0 r_0^2}} \right)}, \\ r_{k+} &= m \left(1 + (-1)^k \sqrt{1 - \frac{a^2}{m^2} - \frac{3r_0}{2m}} \right). \end{aligned} \quad (70)$$

where $k = 1$ indicates the smaller radius, while $k = 2$ indicates the largest radius, and the negative roots were disregarded since the radial coordinate is assumed to be positive.

By inspecting the expressions for the roots just given, and taking into account that the free parameters m/r_0 and a/r_0 are nonnegative, we can see that r_{1-} is complex for all nonvanishing values of the free parameters. Hence, the interior solution can have at most one horizon. This happens if the root r_{2-} is such that $r_{2-} \leq r_0$. Moreover, the complete solution can have at most two horizons. To see this, let us consider the limiting case given by $\Delta_-(r = r_0) = \Delta_+(r = r_0) = 0$, which yields the limiting mass

$$\frac{m_l}{r_0} = 2 \left(1 + \frac{a^2}{r_0^2} \right). \quad (71)$$

For $m/r_0 > m_l/r_0$, the inner Cauchy horizon is located in the interior region with the exterior horizon outside matter. For $m/r_0 = m_l/r_0$, the inner Cauchy horizon is located at the boundary of the object and the exterior located outside the matter. Whereas, for $m/r_0 < m_l/r_0$, the complete solution can present two, one or none horizon outside matter. The extremal case that separates the spacetime with no horizon from a spacetime with two horizons is the extremal case, which is equivalent to the discriminant of $\Delta_+(r)$ vanishing, yielding the extremal mass m_{c+}

$$\frac{m_{c+}}{r_0} = \frac{3}{4} \left(1 + \sqrt{1 + \frac{16 a^2}{9 r_0^2}} \right). \quad (72)$$

The locations of the ergosurfaces that arises in the rotating version of the L&Z charged solution can also be obtained analytically, and are given by similar expressions as Eq. (70), just by replacing a^2 with $a^2 \cos^2 \theta$, what yields

$$\begin{aligned} r_{k-}(\theta) &= r_0 \sqrt{\frac{r_0}{m} \left(1 + (-1)^k \sqrt{1 + \frac{2m a^2 \cos^2 \theta}{r_0 r_0^2}} \right)}, \\ r_{k+}(\theta) &= m \left(1 + (-1)^k \sqrt{1 - \frac{a^2 \cos^2 \theta}{m^2} - \frac{3r_0}{2m}} \right). \end{aligned} \quad (73)$$

The situation for the ergosurface solutions $r_{k\mp}(\theta)$ is similar to that for the horizons $r_{k\mp}$.

Owing the locations of horizons (70) and ergosurfaces (73), we may draw a set of statements regarding the different kinds of objects that the present geometry allows.

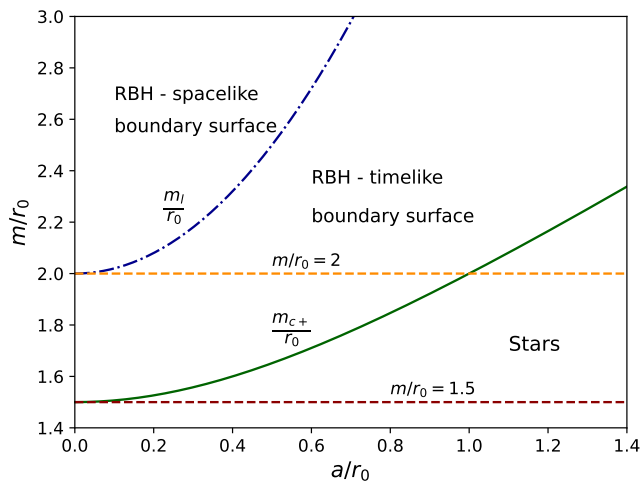


Figure 2. A plot showing the limiting and extremal masses as a function of a/r_0 . The label on each curve indicates the respective normalized mass. Such mass functions are needed in order to uncover the different kinds of objects and the properties of the boundary surfaces. The horizontal lines $m/r_0 = 2$ and $m/r_0 = 1.5$ are important to establish the existence and location of ergosurfaces.

The main classes of objects are the same as the those described in our related work [45], and we give a brief description of them next. Figure 2 summarizes the situation here.

In the interval of large masses, characterized by $m/r_0 > m_l/r_0$ and located in the region above the dashed-dotted line $m/r_0 = m_l/r_0$ in Fig. 2, the complete solution presents two horizons with the inner Cauchy horizon inside matter, while the exterior (event) horizon is located outside matter, representing charged rotating nonextremal RBH with a spacelike boundary. In the lower limit of large masses, i.e., for $m/r_0 = m_l/r_0$, the solution presents two horizons with the inner Cauchy horizon at the boundary of the matter distribution object and the exterior (event) horizon located outside matter, representing charged rotating nonextremal RBH with a lightlike boundary. In the interval of intermediate masses, characterized by $m_{c+}/r_0 < m/r_0 < m_l/r_0$ and corresponding to the region delimited by the solid line $m/r_0 = m_{c+}/r_0$ and the dashed-dotted line $m/r_0 = m_l/r_0$ in Fig. 2, the solutions present the two horizons outside matter, representing charged rotating nonextremal RBH with a timelike boundary. In the lower limit of intermediate masses, i.e., for $m/r_0 = m_{c+}/r_0$, the solution presents a degenerate horizon outside matter, representing charged rotating extremal RBH with a timelike boundary. Finally, in the interval of small masses, characterized by masses in the interval $m/r_0 < m_{c+}/r_0$ and corresponding to the region below the $m/r_0 = m_{c+}/r_0$ in Fig. 2, the solution presents no horizons, representing charged overextremal rotating star-like configurations with a timelike boundary.

Regarding the existence and location of ergosurfaces,

we may draw the following statements.

Configurations characterized by parameters belonging to the regions above the dashed line $m/r_0 = 2$ in Fig. 2 present two ergosurfaces. That region includes charged rotating RBH with a spacelike boundary, charged rotating RBH with a lightlike boundary, charged rotating RBH with a timelike boundary, and star-like objects. Charged rotating nonextremal RBH with a spacelike boundary and a lightlike boundary present the inner ergosurface completely inside matter, while the outer ergosurface is located completely outside matter. Charged rotating nonextremal and extremal RBH with a timelike boundary present the inner ergosurface extending from inside to outside matter, while the outer ergosurface is located completely outside matter. The configurations representing star-like objects present both ergosurfaces extending from the interior to the exterior spacetime regions.

Configurations characterized by parameters belonging to the region between the two dashed lines $m/r_0 = 1.5$ and $m/r_0 = 2$ in Fig. 2, which encompasses charged rotating nonextremal and extremal RBH with a timelike boundary and star-like objects, the configurations present the two ergosurfaces completely outside the matter distribution.

Finally, configurations characterized by parameters belonging to the region below the dashed line $m/r_0 = 1.5$ in Fig. 2, which encompasses stars-like objects, the configurations present no ergosurfaces.

V. CONCLUSIONS

In this work, we obtained and described the rotating version of L&Z electrically charged solution. This rotating version consists of a Kerr-Newman exterior geometry outside a rotating de Sitter core with a rotating electrically charged shell. In order to achieve this task, we revealed the fact that a well-behaved electromagnetic field within the interior region is unattainable without a nonzero current density, unless the electromagnetic fields vanishes entirely within the interior region. In contrast to the static L&Z solution, the complete absence of electromagnetic field within the interior results in discontinuities in the tangential components of the Faraday-Maxwell tensor across the boundary.

Moreover, we have shown that, despite preserving the overall electric charge of the static systems, the flexibility of the Newman-Janis and Gürses-Gürsey procedures in constructing the Faraday-Maxwell tensor enables the existence of different electromagnetic fields, alongside distinct charge densities within the rotating shell, that can be matched with the Kerr-Newman exterior electromagnetic field. In particular, we constructed two different interior electromagnetic fields leading to different current densities within the rotating shell. In the first case, reported in Sec. IV, the gauge potential and the Faraday-Maxwell tensor depend only on the polar coordinate θ ,

leading to a nonvanishing current density within the shell. We showed, despite the nonzero current density, the net charge in the interior of any spheroid of constant $r < r_0$ is zero, as is the total charge within the rotating shell, which is instead concentrated solely on the boundary shell. We interpret the nonzero interior current density as if the fluid has been electrically polarized due to the presence of charged rotating spheroidal shell with the internal medium behaving as a perfect conductor. In the second case, described in Appendix B, the gauge potential and the Faraday-Maxwell tensor depend on both coordinates r and θ , also leading to a nonvanishing current density within the shell. In this case, the net charge contained in the interior of any spheroid of constant $r < r_0$ is nonzero, and depends on the coordinate r . The boundary shell also contributes to the electric charge, so that the total charge of the geometry is the same as for the static seed metric. We interpret this situation as if the total electric charge comes from the interior region, with the rotating fluid also being electrically polarized and behaving as a non-isotropic conductor.

Furthermore, we performed a comprehensive analysis into the properties of the charged rotating geometry, encompassing curvature regularity, energy-momentum tensor, and energy conditions. The investigation unveiled a spectrum of charged objects such as charged rotating RBH with a spacelike boundary, charged rotating RBH with a lightlike boundary, charged rotating RBH with a timelike boundary, charged rotating RBH with a timelike boundary, and overextremal regular star-like objects with a timelike boundary. It is worth mentioning that charged nonextremal RBH with a spacelike boundary are not allowed within the static L&Z electrically charged solutions.

ACKNOWLEDGMENTS

We thank J. P. S. Lemos for stimulating discussions. MLWB is funded by Fundação de Amparo à Pesquisa do Estado de São Paulo (FAPESP), Brazil, Grant No. 2022/09496-8. VTZ is partly funded by Conselho Nacional de Desenvolvimento Científico e Tecnológico (CNPq), Brazil, Grant No. 311726/2022-4, and by Fundação de Aperfeiçoamento do Pessoal de Nível Superior (CAPES), Brazil, Grant No. 88887.310351/2018-00. VTZ thanks Center for Astrophysics and Gravitation (CENTRA), Instituto Superior Técnico, for hospitality.

Appendix A: Fundamental equations

The investigation of this work focuses on compact objects characterized by the Einstein-Maxwell field equations incorporating electrically charged matter. Therefore, in this section, we revised the fundamental equations that are needed for our investigation. These equa-

tions are expressed as follows

$$G_{\mu\nu} = 8\pi T_{\mu\nu} = 8\pi (E_{\mu\nu} + M_{\mu\nu}), \quad (\text{A1})$$

$$\nabla_\nu F^{\mu\nu} = 4\pi J^\mu, \quad (\text{A2})$$

$$\nabla_\alpha F_{\mu\nu} + \nabla_\nu F_{\alpha\mu} + \nabla_\mu F_{\nu\alpha} = 0. \quad (\text{A3})$$

Here, Greek indices range from 0 to 3. The left-hand side of Eq. (A1) consists of the Einstein tensor $G_{\mu\nu} = R_{\mu\nu} - \frac{1}{2}g_{\mu\nu}\mathcal{R}$, where $R_{\mu\nu}$ denotes the Ricci tensor, $g_{\mu\nu}$ represents the metric tensor, and \mathcal{R} signifies the Ricci scalar. Additionally, Eqs. (A2) and (A3) involves the Faraday-Maxwell tensor $F^{\mu\nu}$, which can be expressed using the gauge vector potential \mathcal{A}_μ as $F_{\mu\nu} = \nabla_\mu \mathcal{A}_\nu - \nabla_\nu \mathcal{A}_\mu$, with ∇_μ representing the covariant derivative compatible with the four-dimensional Lorentzian metric. Additionally, J^μ denotes the current density.

The energy-momentum tensor (EMT) $T_{\mu\nu}$ has two components and can be expressed as $T_{\mu\nu} = E_{\mu\nu} + M_{\mu\nu}$. The former stems from the electromagnetic field, while the latter originates from the matter itself.

The electromagnetic EMT $E_{\mu\nu}$ takes the form

$$E_{\mu\nu} = \frac{1}{4\pi} \left(F_{\mu\alpha} F_\nu^\alpha - \frac{1}{4} g_{\mu\nu} F_{\alpha\beta} F^{\alpha\beta} \right). \quad (\text{A4})$$

Meanwhile, the form of the matter EMT $M_{\mu\nu}$ depends on whether the object is rotating or not. In the static case, where the matter content is a perfect fluid with electric charge $M_{\mu\nu} = (\rho_m + p) u^\mu u^\nu + p g_{\mu\nu}$, but the form of the EMT of a charged rotating fluid is not so simple, since rotation breaks isotropy, but, in general, such EMT may be written in the form $M_{\mu\nu} = (\rho_m + p) u^\mu u^\nu + p g_{\mu\nu} + \sigma_{\mu\nu}$.

The last important equation for the our investigation is the conservation of the energy-momentum tensor, namely,

$$\nabla_\nu T^{\mu\nu} = 0. \quad (\text{A5})$$

Appendix B: An alternative electromagnetic field for the rotating Lemos-Zanchin electrically charged solution

1. The interior electromagnetic field

Following the same procedure as described in Sec. II A of Ref. [45], an alternative interior solution for the electromagnetic gauge potential is given by

$$\mathcal{A}_\mu = -\frac{Q(r)r}{\Sigma} (\delta_\mu^t - a \sin^2 \theta \delta_\mu^\varphi), \quad (\text{B1})$$

where the charge function $Q(r)$ is related to the total electric charge inside a spheroid defined by $r = \text{constant}$, as showed in Ref. [45]. This gauge potential has the same form as the the electromagnetic gauge potential of the Kerr-Newman solution, but here with the constant charge q replaced with an arbitrary charge function $Q(r)$.

The gauge potential (B1) leads to the following non-trivial components for the Faraday-Maxwell tensor

$$\begin{aligned} F_{rt} &= \frac{Q(r)(r^2 - a^2 \cos^2 \theta)}{\Sigma^2} - \frac{r Q'(r)}{\Sigma}, \\ F_{\theta t} &= -\frac{Q(r) r a^2 \sin 2\theta}{\Sigma^2}, \\ F_{r\varphi} &= -a \sin^2 \theta F_{rt}, \\ F_{\theta\varphi} &= -\frac{(r^2 + a^2)}{a} F_{\theta t}. \end{aligned} \quad (\text{B2})$$

The simplest nonconstant charge function is

$$Q(r) = \frac{qr}{r_0} \quad (\text{B3})$$

for $r \leq r_0$. In this case, the independent components of the Faraday-Maxwell tensor simplifies to

$$F_{rt} = -\frac{2qra^2 \cos^2 \theta}{r_0 \Sigma^2}, \quad F_{\theta t} = -\frac{qr^2 a^2 \sin 2\theta}{r_0 \Sigma^2}, \quad (\text{B4})$$

which vanishes in the limit $a \rightarrow 0$, recovering the static solution. From Eq. (46), we can see that the electric and magnetic fields, as measured by the comoving observer, are parallel to each other and given by

$$E_r = -\sqrt{\frac{\Sigma}{\pm \Delta}} \frac{2qra^2 \cos^2 \theta}{r_0 \Sigma^2}, \quad (\text{B5})$$

$$B_r = \sqrt{\frac{\Sigma}{\pm \Delta}} \frac{2qr^2 a \cos \theta}{r_0 \Sigma^2}. \quad (\text{B6})$$

In this alternative solution for the interior electromagnetic field, the electric field does not vanish. Hence, in this case the medium does not correspond to a perfect conductor, which differs from the properties of the internal medium found by Tiomno [44].

The current density generated by the Faraday-Maxwell field (B2) is given by

$$4\pi J^t = \frac{2qa^2}{r_0} \left(\frac{r^2 \sin^2 \theta - (r^2 + a^2) \cos^2 \theta}{\Sigma^3} \right), \quad (\text{B7})$$

$$4\pi J^\varphi = \frac{2qa}{r_0} \left(\frac{r^2 - a^2 \cos^2 \theta}{\Sigma^3} \right), \quad (\text{B8})$$

with the other components being identically zero. Let us notice that J^t may change its sign, being positive for $\tan^2 \theta > (r^2 + a^2)/a^2$ and negative for $\tan^2 \theta < (r^2 + a^2)/a^2$, which means that we can interpret the interior fluid as an electrically polarized medium. Moreover, as it seen from Eqs. (B7) and (B8), the two nontrivial components of the current density are finite everywhere in the interior region, with the exception of the ring S^1 , where both components diverge. Inside the ring, at the disc ($r = 0$, $0 \leq \theta < \pi/2$), the two components of the current density are finite and given by $J^t = -2q/r_0 a^2 \cos^4 \theta$ and $J^\varphi = -2q/r_0 a^3 \cos^4 \theta$, respectively. On the other hand, the Faraday-Maxwell tensor given by (B2), with

$Q(r) = qr/r_0$, is finite everywhere inside the fluid and vanishes on the disk and on the ring.

The decomposition of the current density J^μ along the Carter tetrad, given by Eq. (54), allow us to obtain

$$\rho_e = -\sqrt{\frac{\pm \Delta}{\Sigma}} \frac{qa^2 \cos^2 \theta}{2\pi r_0 \Sigma^2}, \quad (\text{B9})$$

$$j^\mu = \frac{qr^2}{2\pi r_0 \Sigma^2} \frac{a \sin \theta}{\sqrt{\Sigma}} e_3^\mu, \quad (\text{B10})$$

where e_3^μ is the fourth component of the Carter tetrad. Since the medium does not correspond to a perfect conductor and the conduction current j^μ does not vanish, we can associate the internal electric field to the conduction current through the following well-known (see e.g. [51]) relation

$$j^\mu = \kappa^{\mu\nu} E_\nu, \quad (\text{B11})$$

where $\kappa^{\mu\nu}$ is the symmetrical conductivity tensor which, in the present case, is given by

$$\kappa^{\mu\nu} = -\frac{r \sin \theta}{4\pi a \sqrt{\Sigma} \cos^2 \theta} e_1^\mu e_3^\nu. \quad (\text{B12})$$

Hence, we can interpret this medium as a non-isotropic conductor given that the conduction current does not flow in the same direction of the electric field.

At last, we calculate the net electric charge in the interior of the spheroidal surface of constant radius $r = r_0$. Equation (48) furnishes

$$q(r_0) = q - \frac{q}{r_0} \frac{r_0^2 + a^2}{a} \arctan \frac{a}{r_0}, \quad (\text{B13})$$

where the last term of the equation above comes from the last term of Eq. (48) once $Q'(r_0) = q \neq 0$.

2. The exterior electromagnetic field

For $r > r_0$, the electromagnetic gauge potential and the Faraday-Maxwell tensor are given by Eqs. (59) and (60), respectively. Therefore, the exterior solution is, as expected, the well-known Kerr-Newman electromagnetic fields.

3. Matching conditions for the electromagnetic field

The matching conditions are given by $[A_a] = 0$, $[F_{ab}] = 0$ and $[F_{an}] = 4\pi \sigma_e u_a$, where σ_e is the surface charge density of the shell and u^a is the four-velocity of the boundary given by 0–element of the tetrad in Eq. (38). It is straightforward to see that the first two conditions are trivially satisfied while the last condition give us the

charge density of the shell as measured by an observer comoving with the boundary, i.e.,

$$\sigma_e = \frac{q}{4\pi (r_0^2 + a^2 \cos^2 \theta)}. \quad (\text{B14})$$

Notice that the result for the static solution (9) is recovered in the limit $a = 0$.

The integration of the charge density (B14) over the surface $r = r_0$ gives us

$$q_s(r_0) = \frac{q}{r_0} \frac{r_0^2 + a^2}{a} \arctan \frac{a}{r_0}. \quad (\text{B15})$$

Thus, combining Eqs. (B13) and (B15), we can see that the total electric charge of the complete solution is q , i.e., $q(r_0) + q_s(r_0) = q$. Therefore, in contrast to the case discussed in the main text, the total electric charge comes from the interior region.

-
- [1] J. M. Bardeen, Non-singular general-relativistic gravitational collapse, in *Abstracts of the 5th International Conference on Gravitation and the Theory of Relativity*, edited by V. A. Fock (Tbilisi University Press, Tbilisi, 1968), p. 174.
- [2] E. Ayón-Beato and A. García, The Bardeen model as a nonlinear magnetic monopole, *Phys. Lett. B* **493**, 149 (2000).
- [3] V. P. Frolov, M. A. Markov, and V. F. Mukhanov, Through a black hole into a new universe?, *Phys. Lett. B* **216**, 272 (1989).
- [4] I. G. Dymnikova, Vacuum nonsingular black hole, *Gen. Relativ. Gravit.* **24**, 235 (1992).
- [5] K. A. Bronnikov, Regular magnetic black holes and monopoles from nonlinear electrodynamics, *Phys. Rev. D* **63**, 044005 (2001).
- [6] I. Dymnikova, Regular electrically charged structures in nonlinear electrodynamics coupled to general relativity, *Classical Quantum Gravity* **21**, 4417 (2004).
- [7] S. A. Hayward, Formation and evaporation of nonsingular black holes, *Phys. Rev. Lett.* **96**, 031103 (2006).
- [8] K. A. Bronnikov and J. C. Fabris, Regular phantom black holes, *Phys. Rev. Lett.* **96**, 251101 (2006).
- [9] O. B. Zaslavskii, Regular black holes and energy conditions, *Phys. Lett. B* **688**, 278 (2010).
- [10] J. P. S. Lemos and V. T. Zanchin, Regular black holes: Electrically charged solutions, Reissner-Nordström outside a de Sitter core, *Phys. Rev. D* **83**, 124005 (2011).
- [11] J. P. S. Lemos and V. T. Zanchin, Regular black holes: Guilfoyle electrically charged solutions with a perfect fluid phantom core, *Phys. Rev. D* **93**, 124012 (2016).
- [12] Z.-Y. Fan and X. Wang, Construction of regular black holes in general relativity, *Phys. Rev. D* **94**, 124027 (2016).
- [13] A. D. D. Masa, E. S. de Oliveira, and V. T. Zanchin, New regular black hole solutions and other electrically charged compact objects with a de Sitter core and a matter layer, *Int. J. Mod. Phys. D* **27** 11 (2018).
- [14] A. Simpson and M. Visser, Regular black holes with asymptotically Minkowski cores, *Universe* **6**, 8 (2019).
- [15] M. Gürses and F. Gürsey, Lorentz covariant treatment of the Kerr-Schild geometry, *J. Math. Phys.* **16**, 2385 (1975).
- [16] E. T. Newman and A. I. Janis, Note on the Kerr spinning particle metric, *J. Math. Phys.* **6**, 915 (1965).
- [17] A. Burinskii, E. Elizalde, S. R. Hildebrandt, and G. Magli, Regular sources of the Kerr-Schild class for rotating and nonrotating black hole solutions, *Phys. Rev. D* **65**, 064039 (2002).
- [18] P. Beltracchi and P. Gondolo, Physical interpretation of Newman-Janis rotating systems. I. A unique family of Kerr-Schild systems, *Phys. Rev. D* **104**, 124066 (2021).
- [19] S. P. Drake and P. Szekeres, Uniqueness of the Newman-Janis algorithm in generating the Kerr-Newman metric, *Gen. Relativ. Gravit.* **32**, 445 (2000).
- [20] C. Bambi and L. Modesto, Rotating regular black holes, *Phys. Lett. B* **721**, 329 (2013).
- [21] M. Azreg-Aïnou, Generating rotating regular black hole solutions without complexification, *Phys. Rev. D* **90**, 064041 (2014).
- [22] A. Smailagic and E. Spallucci, "Kerr" black hole: The lord of the string, *Phys. Lett. B* **688**, 82 (2010).
- [23] L. Modesto and P. Nicolini, Charged rotating noncommutative black holes, *Phys. Rev. D* **82**, 104035 (2010).
- [24] B. Toshmatov, B. Ahmedov, A. Abdujabbarov, and Z. Stuchlik, Rotating regular black hole solution, *Phys. Rev. D* **89**, 104017 (2014).
- [25] J. C. S. Neves and A. Saa, Regular rotating black holes and the weak energy condition, *Phys. Lett. B* **734**, 44 (2014).
- [26] I. Dymnikova and E. Galaktionov, Regular rotating electrically charged black holes and solitons in non-linear electrodynamics minimally coupled to gravity, *Classical Quantum Gravity* **32**, 165015 (2015).
- [27] B. Toshmatov, Z. Stuchlik, and B. Ahmedov, Generic rotating regular black holes in general relativity coupled to nonlinear electrodynamics, *Phys. Rev. D* **95** (2017).
- [28] R. Torres and F. Fayos, On regular rotating black holes, *Gen. Relativ. Gravit.* **49**, 2 (2017).
- [29] S. G. Ghosh, M. Amir, and S. D. Maharaj, Ergosphere and shadow of a rotating regular black hole, *Nucl. Phys. B* **957**, 115088 (2020).
- [30] J. Mazza, E. Franzin, and S. Liberati, A novel family of rotating black hole mimickers, *J. Cosmol. Astropart. Phys.* **04** 082, (2021).
- [31] E. Franzin, S. Liberati, J. Mazza, and V. Vellucci, Stable rotating regular black holes, *Phys. Rev. D* **106**, 104060 (2022).
- [32] A. D. Masa and V. T. Zanchin, Rotating regular black holes and other compact objects with a Tolman-type potential as a regular interior for the Kerr metric, *Int. J. Mod. Phys. D* **33**, 2350102 (2024).

- [33] R. Brustein and A. J. M. Medved, Sourcing the Kerr geometry, [arXiv:2310.16467](#) (2023).
- [34] I. Dymnikova, *Regular rotating black holes and solitons with the de Sitter/phantom interiors*, contained in C. Bambi, *Regular black holes* (Springer, Singapore, 2023).
- [35] R. Ghosh, M. Rahman, and A.K. Mishra, Regularized stable Kerr black hole: cosmic censorship, shadow and quasi-normal modes, *Eur. Phys. J. C* **83**, 91 (2023).
- [36] H. Maeda, Quest for realistic non-singular black-hole geometries: Regular-center type. *J. High Energ. Phys.* **2022**, 108 (2022).
- [37] R. Torres, Regular rotating black holes: A review, [arXiv:2208.12713](#) (2022).
- [38] R. Torres, Interiors of singularity-free rotating black holes, *Phys. Rev. D* **108**, 084008 (2023).
- [39] T. Zhou and L. Modesto, On the analytic extension of regular rotating black holes, [arXiv:2303.11322](#) (2023).
- [40] R. P. Kerr, Gravitational field of a spinning mass as an example of algebraically special metrics, *Phys. Rev. Lett.* **11**, 237 (1963).
- [41] B. O'Neill, *The geometry of Kerr black holes* (Dover Publications, New York, 1995).
- [42] M. Azreg-Aïnou, Regular and conformal regular cores for static and rotating solutions, *Phys. Lett. B* **730**, 95 (2014).
- [43] E. T. Newman, E. Couch, K. Chinnapared, A. Exton, A. Prakash, and R. Torrence, Metric of a rotating, charged mass, *J. Math. Phys.* **6**, 918 (1965).
- [44] J. Tiomno, Electromagnetic field of rotating charged bodies, *Phys. Rev. D* **7**, 992 (1973).
- [45] M. L. W. Basso and V. T. Zanchin, Compact regular objects from an electrified Tolman-like density: A new interior region for the Kerr-Newman spacetime, [arXiv:2406.13032](#) (2024).
- [46] D. Lynden-Bell, Electromagnetic magic: The relativistically rotating disk, *Phys. Rev. D* **70**, 105017 (2004).
- [47] J. R. Gair and D. Lynden-Bell, Electromagnetic fields of separable spacetimes, *Classical Quantum Gravity* **24**, 1557 (2007).
- [48] C. G. Tsagas, Electromagnetic fields in curved spacetimes, *Classical Quantum Gravity* **22**, 393 (2005).
- [49] I. Dymnikova, E. Galaktionov, Generic behavior of electromagnetic fields of regular rotating electrically charged compact objects in nonlinear electrodynamics minimally coupled to gravity, *Symmetry* **15**, 188 (2023).
- [50] W. Israel, Singular hypersurfaces and thin shells in general relativity, *Nuovo Cimento* **44B**, 1 (1966); Corrections in **48B**, 463 (1967).
- [51] J. D. Bekenstein and E. Oron, New conservation laws in general-relativistic magnetohydrodynamics, *Phys. Rev. D* **18**, 1809 (1978).